

# SnoopLigase catalyzes peptide-peptide locking and enables solid-phase conjugate isolation

Can M Buldun,<sup>†,||</sup> Jisoo X Jean,<sup>†,||</sup> Michael R Bedford<sup>‡</sup> and Mark Howarth<sup>†\*</sup>

<sup>†</sup>Department of Biochemistry, University of Oxford, South Parks Road, Oxford, OX1 3QU, UK.

<sup>‡</sup>AB Vista, Woodstock Court, Marlborough, SN8 4AN, UK.

\*Correspondence and requests for materials should be addressed to M.H. (email: mark.howarth@bioch.ox.ac.uk).

## Abstract

Simple efficient reactions for connecting biological building-blocks open up many new possibilities. Here we have designed SnoopLigase, a protein which catalyzes site-specific transamidation, forming an isopeptide bond with more than 95% efficiency between two peptide tags, SnoopTagJr and DogTag. We initially developed these components by three-part splitting of the *Streptococcus pneumoniae* adhesin RrgA. The units were then engineered, guided by structure, bioinformatic analysis of sequence homology, and computational prediction of stability. After engineering, SnoopLigase demonstrated high yield coupling under a wide range of buffers and temperatures. SnoopTagJr and DogTag were functional at the N- or C-terminus, while DogTag was also functional at internal sites in proteins. Having directed reaction of SnoopTagJr and DogTag, SnoopLigase remained stably bound to the ligated product, so reconstituting the parent domain. Separating products from unreacted starting material and catalyst is often as challenging as reactions themselves. However, solid-phase immobilization of SnoopLigase enabled the ligated SnoopTagJr-DogTag product to be eluted with high purity, free from SnoopLigase or unligated substrates. The solid-phase catalyst could then be re-used multiple times. In search of a generic route to improve the resilience of enzymes, we fused SnoopTagJr to the N-terminus and DogTag to the C-terminus of model enzymes, allowing cyclization via SnoopLigase. While wild-type phytase and  $\beta$ -lactamase irreversibly aggregated upon heating, cyclization using SnoopLigase conferred exceptional thermoresilience, with both enzymes retaining solubility and activity following heat treatment up to 100 °C. SnoopLigase should create new opportunities for conjugation and nanoassembly, while illustrating how to harness product inhibition and extend catalyst utility.

## Introduction

Deepening our insight into the complexity of living systems will depend on having freedom to arrange components in arbitrary combinations or architectures. Site-specifically functionalized proteins open up a variety of avenues, such as stable single-molecule imaging,<sup>1</sup> targeting toxins to specific cell-types,<sup>2</sup> and improving the circulation of protein drugs.<sup>3-4</sup> Proteins are the biomolecules with the widest range of

functional activities and the use of peptide tags is a powerful approach for controlling protein function. Peptide tags are simple to encode genetically and their small size reduces the interference with natural interactions, the cost of biosynthesis, and the immunogenicity.<sup>5</sup>

Here we sought to design a generally-applicable new catalyst for joining one peptide tag to another peptide tag irreversibly with high yield. We wanted all components to be composed of the regular 20 amino acids<sup>6</sup> for easy use in any cellular system, but excluding cysteine for application in oxidizing or reducing compartments. Our inspiration was the intramolecular isopeptide bond formation of certain Gram-positive bacterial surface proteins.<sup>7</sup> We previously split FbaB from *Streptococcus pyogenes*, generating SpyLigase, which directed isopeptide bond formation between two peptide tags.<sup>8</sup> SpyLigase was a useful proof of principle, but yield was rarely above 50%.<sup>8-9</sup> We hypothesized that splitting the *Streptococcus pneumoniae* adhesin RrgA would allow peptide-peptide ligation with better thermodynamic driving force, generating ammonia as a product rather than water for SpyLigase.<sup>10-11</sup> SpyLigase reaction also required precise and inconvenient conditions (i.e. 4 °C with 1.5 M trimethylamine N-oxide).<sup>8</sup> We considered that SpyLigase's condition-dependence reflected the fold instability, so that efforts to rigidify the ligase could make a more widely-applicable catalyst.

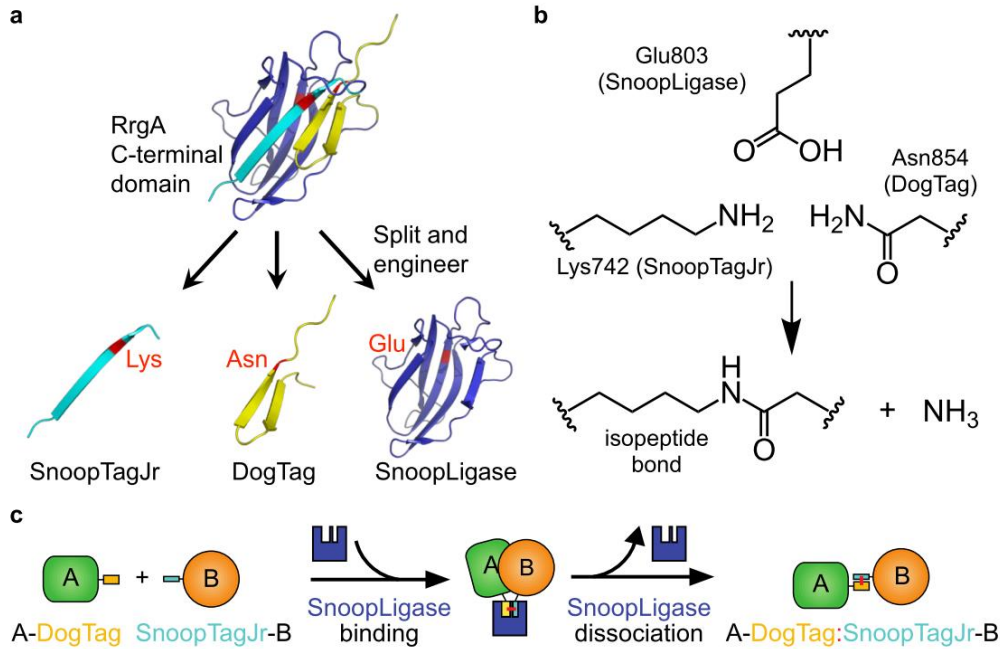
Here we describe the process of dissecting RrgA, followed by structure-based and computational optimization to generate SnoopLigase, a robust technology for peptide-peptide ligation. We establish the tolerance of SnoopLigase to a wide range of buffers and temperatures. SnoopLigase's product inhibition is harnessed to enable clean conjugate purification, a major challenge in bioconjugation chemistry.<sup>3</sup> Then we demonstrate the use of SnoopLigase for head-to-tail ligation of different enzymes, achieving in one step > 60 °C increase in thermal resilience of an enzyme.

## Results and Discussion

**Design principle of the peptide-peptide ligase.** The C-terminal domain of the *Streptococcus pneumoniae* adhesin RrgA contains a spontaneous isopeptide bond between Lys and Asn, promoted by an apposed Glu (Fig. 1A,B).<sup>11</sup> We had previously split this domain into two parts, enabling reaction of the 12 amino acid peptide SnoopTag with the 112 amino acid protein partner SnoopCatcher.<sup>12</sup> This pair was a strong foundation to split the C-terminal domain of RrgA into a trio, such that the residues of the reactive triad were located on three different units, to enable peptide-peptide ligation. After extensive variation of the sites of splitting, we settled on the units SnoopTag (reactive Lys, residues 734-745, 12 amino acids), DogTag (reactive Asn, residues 838-860, 23 amino acids) and RrgA Ligase (catalytic Glu, residues 743-846, 104 amino acids) (Fig 1A, Fig. S1). SnoopTag overlapped for 3 residues with RrgA Ligase, while DogTag overlapped for 9 residues with RrgA Ligase (Fig. S1). The G842T and D848G point mutations in RrgA, previously made to enhance SnoopCatcher reactivity with SnoopTag,<sup>12</sup> were

included in RrgA Ligase and DogTag. Our hypothesis was that the ligase should be able to bind SnoopTag and DogTag and catalyze the formation of the isopeptide bond between the two tags (Fig 1B), thereby mediating covalent conjugation of a SnoopTag fusion protein and a DogTag fusion protein (Fig 1C).

## Figure 1

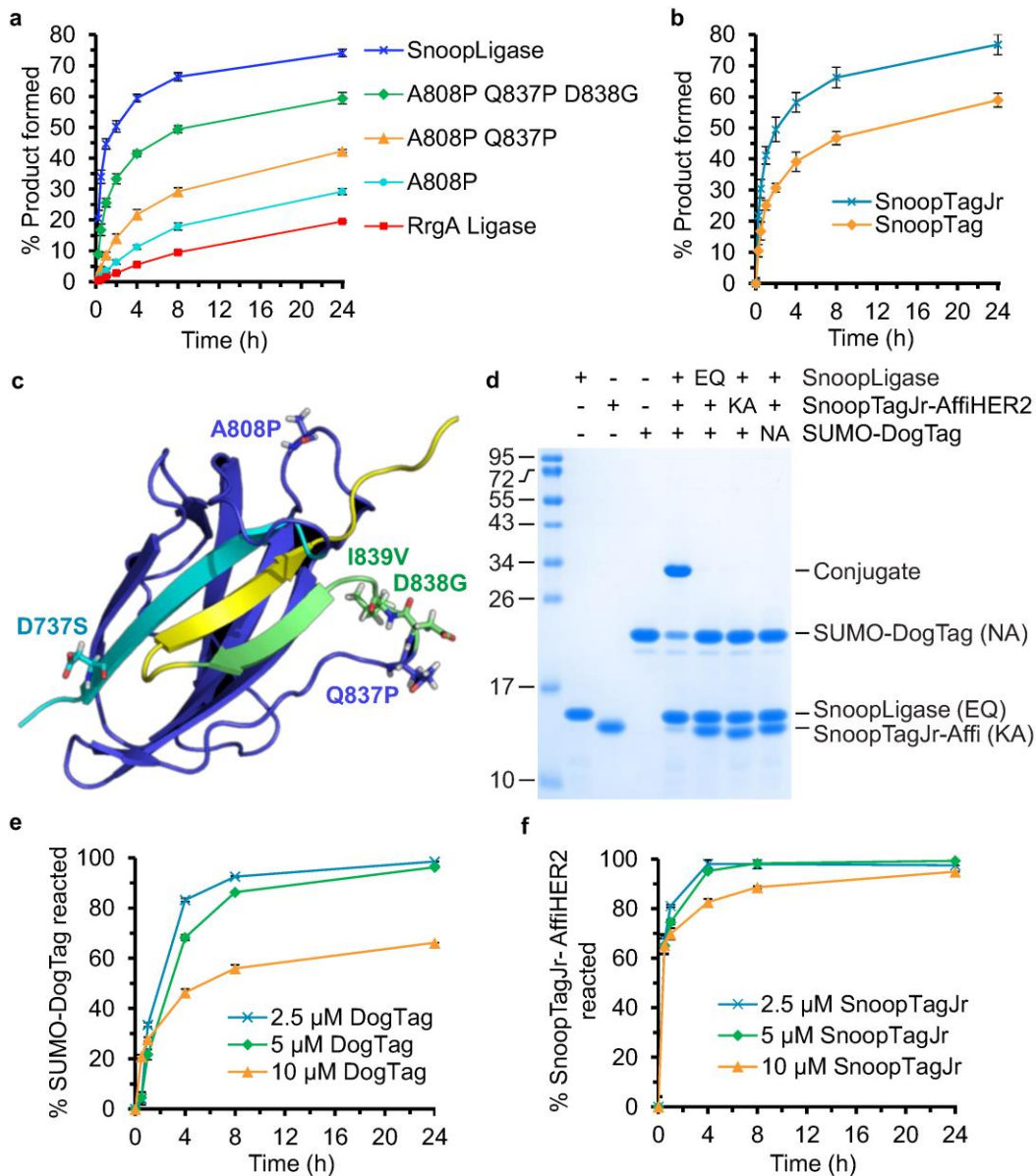


**Figure 1. Design principle of SnoopLigase.** (a) Cartoon of domain splitting. The C-terminal domain of RrgA (Protein Data Bank 2WW8) was split into three parts and engineered, such that the reactive Lys is located on SnoopTagJr (turquoise), the reactive Asn on DogTag (yellow) and the catalytic Glu on SnoopLigase (blue) (key residues highlighted in red). (b) Molecular basis for isopeptide bond formation in RrgA. Glu803 promotes isopeptide bond formation between Lys742 and Asn854, eliminating ammonia. (c) Schematic of the use of SnoopLigase to direct peptide-peptide ligation (the isopeptide bond is represented in red).

**Structure-based and computational optimization of ligation activity.** Removal of three  $\beta$ -strands from a small protein domain is a major modification and it is common for split proteins to have reduced stability.<sup>13</sup> Initial testing found that RrgA Ligase showed low solubility when purified from *Escherichia coli* and only a small percentage of ligation could be obtained, which was restricted to 4 °C and very precise buffer composition. We hypothesized that stabilizing the split domain would be important to enhance ligase performance. We initially sought to engineer  $\beta$ -turns of the protein domain, which are frequently flexible.<sup>14</sup>  $\beta$ -turns may be stabilized by substitution of appropriate residues with proline,<sup>15-16</sup> which has a fixed  $\phi$ -angle of approximately  $-60^\circ$ , limiting the conformational flexibility of the polypeptide backbone. We analyzed each loop of RrgA's C-terminal domain and identified two

promising proline substitutions (A808P and Q837P). To improve ligase stability further, we analyzed the domain computationally, integrating evidence on tolerated mutations from natural homologs of RrgA in the sequence databases, along with atomistic Rosetta modeling for the effect of mutations on fold energetics.<sup>17</sup> Five mutations (D737S, A820E, D830N, D838G, I839V) were taken forward; we did not pursue any suggested mutations adjacent to the isopeptide bond or introducing surface-exposed hydrophobic amino acid side-chains. Most mutations suggested by this analysis improved the fold stability, as computationally predicted by Rosetta (Fig. S2A).<sup>18</sup> Three mutations (D737S, D838G, I839V) substantially improved reaction yield and rate (Fig. 2A, Fig. S2B-D). With the combination of A808P, Q837P, D838G and I839V mutations (termed SnoopLigase), the reaction rate was increased 66-fold over RrgA Ligase (Fig. 2A, Fig. S3). As expected, the Rosetta energy score was also improved (Fig. S3). Similarly, D737S mutation in SnoopTag, termed SnoopTagJr, was also successful in improving reaction (Fig. 2B). The sequences of all tags and ligases are aligned in Fig. S1. We mapped the mutations on the structure of RrgA, illustrating the importance of the loop of SnoopLigase overlapping with DogTag (Fig. 2C).

To validate the proposed route of SnoopLigase reaction, we analyzed peptide-peptide ligation with each of the three key residues mutated. We fused SnoopTagJr to an affibody against the growth factor receptor HER2 (SnoopTagJr-AffiHER2).<sup>19</sup> DogTag was fused with a model domain, small ubiquitin modifier (SUMO). SnoopLigase efficiently ligated SnoopTagJr-AffiHER2 to SUMO-DogTag (Fig. 2D). However, mutation of the Lys in SnoopTagJr, the Asn in DogTag, or the Glu in SnoopLigase abolished product formation (Fig. 2D), consistent with the reactive triad being responsible for covalent adduct formation. SnoopLigase expressed efficiently in *E. coli* (> 10 mg per L of culture) and was highly soluble (> 500  $\mu$ M). At equimolar substrate concentration, SnoopLigase-mediated conjugation reached 60 – 80% substrate conversion after 24 h. Employing excess of the SnoopTagJr-partner and SnoopLigase enabled  $\geq 95\%$  of the DogTag-partner to react (2-fold excess  $96.3 \pm 0.4\%$ ; 4-fold excess  $98.5 \pm 0.3\%$ , mean of triplicate  $\pm 1$  SD) (Fig. 2E, Fig. S4). Similarly, excess of the DogTag-partner and SnoopLigase enabled  $\geq 95\%$  of the SnoopTagJr-partner to react (2-fold excess  $99.3 \pm 0.3\%$ ; 4-fold excess  $97.5 \pm 1.7\%$ , mean of triplicate  $\pm 1$  SD) (Fig. 2F, Fig. S4). Kinetic analysis for SnoopLigase revealed  $K_M$  values of  $8.4 \pm 1.4 \mu$ M for SnoopTagJr-AffiHER2 and  $11.9 \pm 0.8 \mu$ M for SUMO-DogTag (Fig. S5).

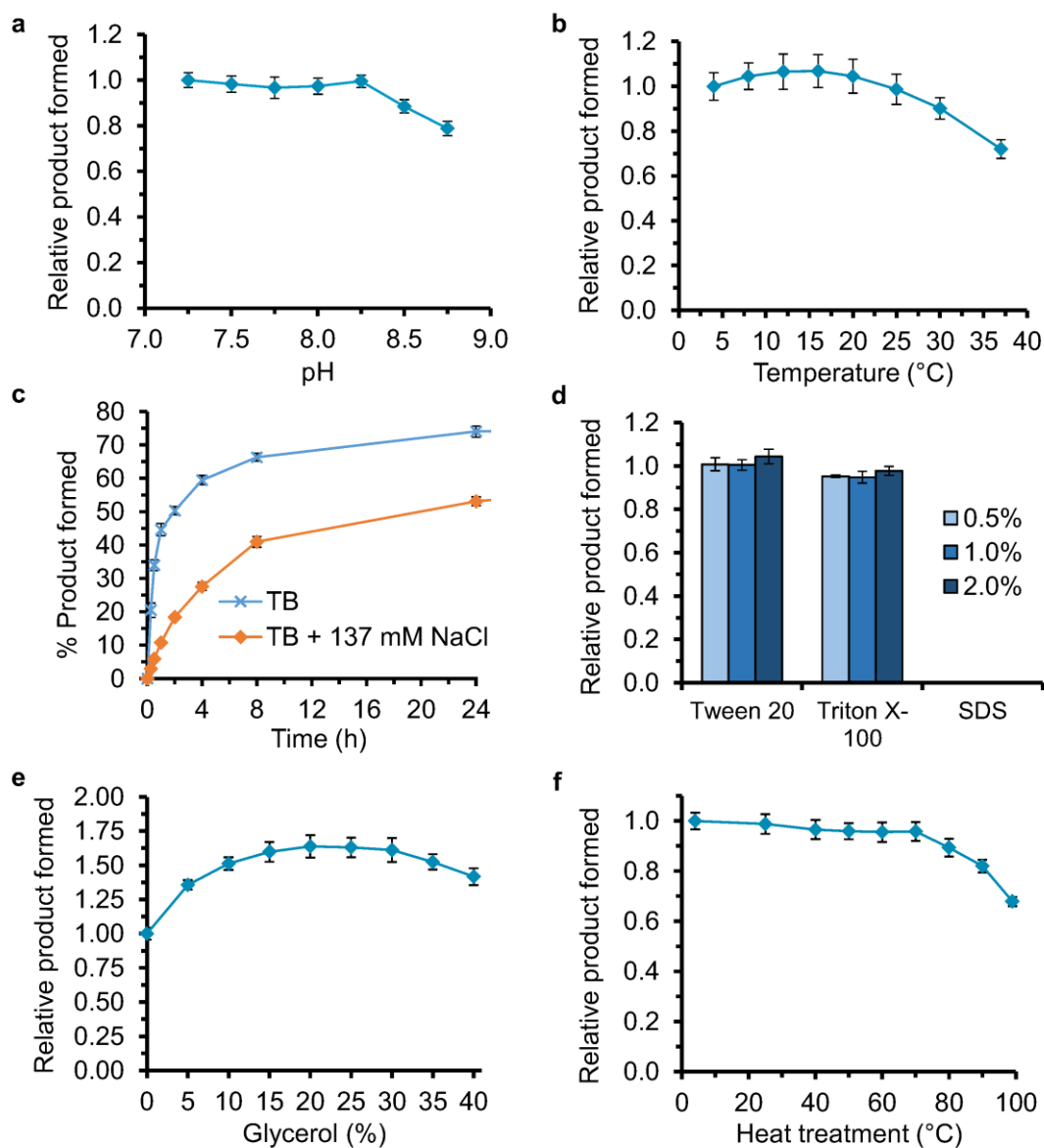
**Figure 2**

**Figure 2. Engineering of SnoopLigase.** (a) Mutations to enhance ligation. 10  $\mu$ M RrgA Ligase, point mutants thereof, or SnoopLigase was incubated with equimolar SnoopTagJr-AffiHER2 and SUMO-DogTag at 4  $^{\circ}$ C and ligated product was determined by SDS-PAGE with Coomassie staining and densitometry. (b) SnoopTag and SnoopTagJr reactivity. SnoopTag- or SnoopTagJr-AffiHER2 (10  $\mu$ M) was incubated with equimolar SUMO-DogTag and SnoopLigase at 4  $^{\circ}$ C. (c) Location of mutated residues enhancing RrgA Ligase (blue) and SnoopTag (turquoise) within RrgA (from PDB 2WW8). Yellow represents DogTag and green the region in both SnoopLigase and DogTag. (d) Specificity of residues in ligation. SnoopLigase was incubated with SnoopTagJr-AffiHER2 and SUMO-DogTag (each 10  $\mu$ M) for 24 h at 4  $^{\circ}$ C, before SDS-PAGE and Coomassie staining. Mutations of key residues in each partner blocked reaction. (e) Maximizing DogTag conjugation. 10  $\mu$ M SnoopTagJr-AffiHER2 and 10  $\mu$ M SnoopLigase were incubated with 2.5-10  $\mu$ M SUMO-DogTag at 4  $^{\circ}$ C. (f) Maximizing SnoopTagJr-

AffiHER2 conjugation. 10  $\mu$ M SUMO-DogTag and 10  $\mu$ M SnoopLigase were incubated with 2.5-10  $\mu$ M SnoopTagJr-AffiHER2 at 4 °C. Error bars are mean  $\pm$  1 SD, n = 3.

To explore the breadth of SnoopLigase substrates, we conjugated four different SnoopTagJr-linked proteins with four different DogTag-linked proteins. Both SnoopTagJr and DogTag were functional as C-terminal or N-terminal fusions. Coupling in most cases proceeded to over 95%, with the lowest yield at 79.5% (Fig. S6). Since DogTag consists of two antiparallel  $\beta$ -strands, we hypothesized that DogTag could be inserted into protein loops. DogTag was inserted with six-residue flexible linkers on either side into HaloTag7 and MBP.<sup>20-21</sup> The DogTag-inserted constructs showed good soluble expression and we found efficient conjugation by SnoopLigase (Fig. S7).

**SnoopLigase was active under diverse conditions.** Having enhanced the activity of the peptide ligase under mild reaction conditions, we then explored SnoopLigase's tolerance to a range of different situations. SnoopLigase reaction functioned well from pH 7.25 to 8.75 (Fig. 3A). Efficient ligation occurred over a wide range of temperatures (4-37 °C) (Fig. 3B). SnoopLigase was functional in the presence of extracellular concentrations of NaCl, although reaction proceeded most efficiently with Tris-borate buffer in the absence of NaCl (Fig. 3C). SnoopLigase reacted well in the presence of the commonly-used detergents Tween 20 and Triton X-100 up to 2%, but sodium dodecyl sulfate (SDS) blocked the reaction (Fig. 3D). Addition of the protein stabilizer glycerol slightly enhanced reaction rate (Fig. 3E). SnoopLigase was also thermoresilient, regaining full activity following heating up to 70 °C (Fig. 3F). Similarly, after lyophilization and storage at 37 °C for 120 days, SnoopLigase retained nearly all of its activity following reconstitution (Fig. S8A). Since there are no cysteines in any of the units, ligation was unaffected by reducing conditions (Fig. S8B).

**Figure 3**

**Figure 3. SnoopLigase reacted over a range of conditions.** (a) pH-dependence. SnoopTagJr-AffiHER2 and SUMO-DogTag were ligated using SnoopLigase (10  $\mu$ M each) for 1.5 h at 4  $^{\circ}$ C in TB + 15% (v/v) glycerol with the indicated pH. (b) Temperature-dependence. As in (a) at pH 7.25 from 4-37  $^{\circ}$ C. (c) Salt-dependence. As in (a) at pH 7.25 with or without additional NaCl. (d) Detergent-dependence. As in (a) at pH 7.25 with 0.5-2% Tween 20, Triton X-100 or SDS. (e) Glycerol-dependence. As in (a) at pH 7.25 with 0-40% glycerol. (f) SnoopLigase was thermoresilient. SnoopLigase was incubated at 4-100  $^{\circ}$ C for 15 min. After cooling, SnoopLigase was used for ligation of SnoopTagJr-AffiHER2 and SUMO-DogTag as in (a) at pH 7.25. Results are mean of triplicate  $\pm$  1 SD.

**SnoopLigase's product inhibition enabled solid-phase conjugate purification.** Having generated an interesting conjugate, one usually then must face the challenge of purifying the conjugate away from the

catalyst and unreacted starting materials. SnoopLigase needed to be present at stoichiometric concentrations for efficient substrate coupling. This makes sense given its origin, where binding of each peptide to SnoopLigase would create a structure similar to the well-folded parent domain. Since SnoopLigase can be easily produced, the demand for high levels of SnoopLigase is not too problematic, but the product inhibition also created an opportunity to simplify substantially the generation of pure conjugate.

Upon reaction, SnoopLigase's strong binding to the reaction product could allow efficient purification of product, free from starting material or SnoopLigase itself (Fig. 4A). After reacting SnoopTagJr-AffiHER2 with SUMO-DogTag using site-specifically biotinylated SnoopLigase, the ligase was captured by streptavidin-agarose resin. The strong interaction between biotin-streptavidin and SnoopLigase-reaction product permitted stringent washing, such that non-reacted and non-immobilized proteins were removed. Incubation of the resin with glycine buffer at pH 2, as commonly used in elution from antibodies,<sup>22</sup> did not affect biotin-streptavidin interaction, but disrupted SnoopLigase-reaction product interaction and yielded high purity ligated product (Fig. 4B).

We also established an alternative solid-phase capture, forming a covalent bond between HaloLink resin and HaloTag7 fused to SnoopLigase. Here we achieved elution with 2 M imidazole at neutral pH to elute selectively the product of SnoopLigase reaction (Fig. S9). Elution from biotin-SnoopLigase was also achieved with 2 M imidazole pH 7.0 (Fig. 4B). To analyze whether this elution condition irreversibly damaged proteins, we tested fluorescence of mEGFP and mKate2, as well as binding activity of HaloTag7SS to HaloLink resin after incubation in 2 M imidazole and dialysis. All proteins fully retained their activity (Fig. S10).

While many proteins survive incubation in pH 2.0 or 2 M imidazole, others may require a milder elution. We hypothesized that elution would be possible using conjugated SnoopTagJr:DogTag peptide to compete out the conjugate of interest from immobilized SnoopLigase. We generated this competitor peptide via SUMO-DogTag and SUMO protease (Fig. S11). Competition using SnoopTagJr:DogTag peptide allowed clean elution of product from biotin-SnoopLigase (Fig. 4B).

Solid-phase purification eliminated the need for subsequent separation of the product from enzyme and unreacted started materials by size exclusion chromatography, which is time-consuming and often leads to substantial losses. In line with the strong binding of SnoopLigase to the product, SnoopLigase could not be separated from the product by size exclusion chromatography (Fig. S12).

Mass spectrometry of the solid-phase purified SUMO-DogTag after SnoopLigase-mediated ligation of SnoopTag peptide gave an increase in molecular weight consistent with the mass of the peptide minus 17 Da from loss of NH<sub>3</sub> (Fig. 4C).

Immobilizing enzymes on solid-phase can improve reaction efficiency and facilitate cost-effective re-use of purified enzymes.<sup>23</sup> To test whether SnoopLigase could be recycled, we immobilized biotin-SnoopLigase on streptavidin-agarose and performed a ligation reaction by addition of SnoopTagJr-AffiHER2 and SUMO-DogTag. Upon washing and elution of the reaction product, the SnoopLigase-coupled agarose was used for another ligation. The amount of product formed remained constant for at least 8 reaction cycles, indicating that SnoopLigase can perform multiple turn-overs and that SnoopLigase resin can be efficiently regenerated (Fig. 4D).

## Figure 4

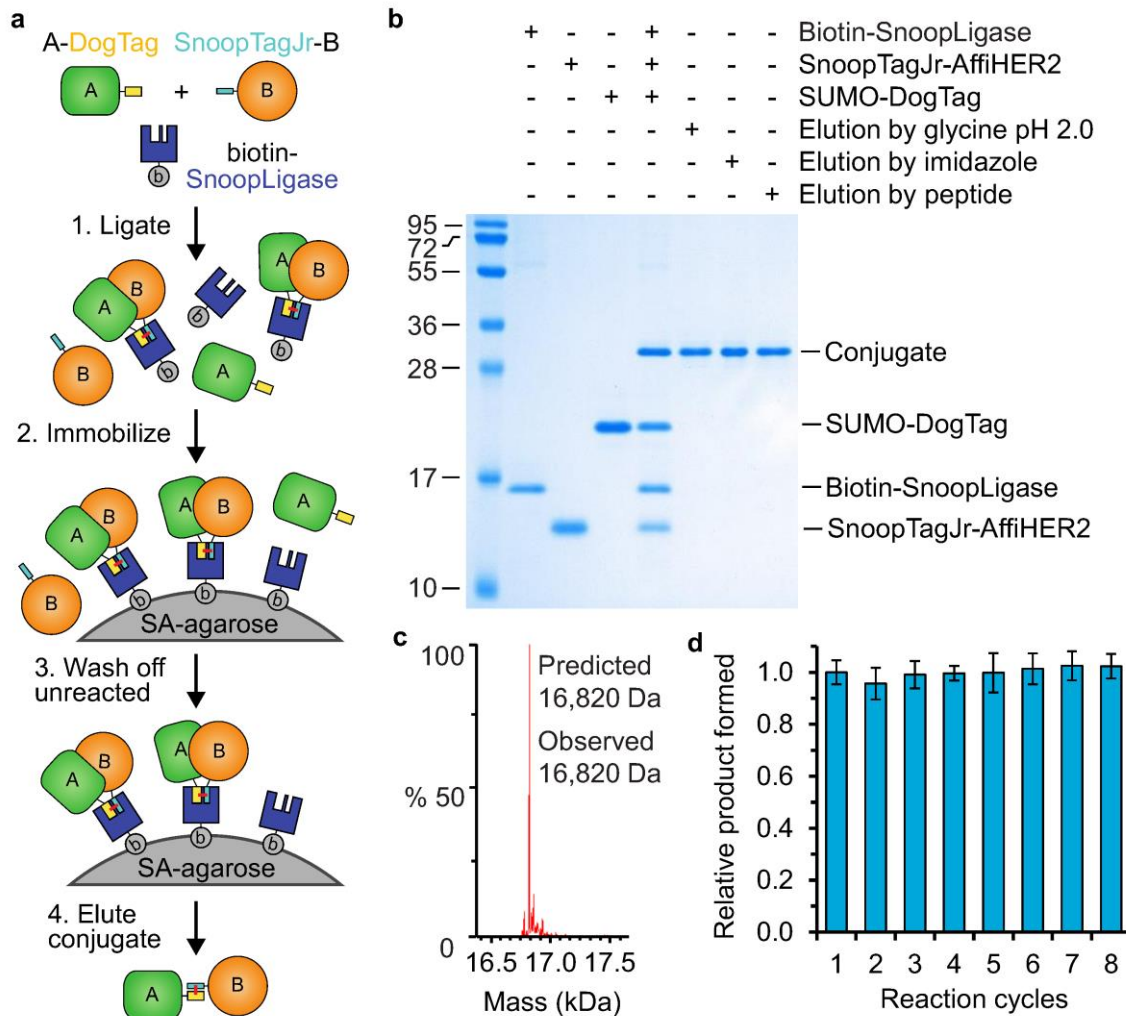


**Figure 4. Purification of SnoopLigase reaction product.** (a) Cartoon of solid-phase SnoopLigase purification. SnoopTagJr- and DogTag-linked proteins are covalently conjugated using biotin-SnoopLigase. Streptavidin-agarose binds biotin-SnoopLigase, unreacted proteins are washed away, and ligated proteins are eluted. (b) Analysis of product from SnoopLigase purification using three different elution methods. SnoopTagJr-AffiHER2 and SUMO-DogTag were ligated using biotin-SnoopLigase (10  $\mu$ M each) for 16 h at 4  $^{\circ}$ C. Biotin-SnoopLigase was captured with streptavidin-agarose, followed by glycine pH 2.0, imidazole or peptide elution procedures. Analysis by SDS-PAGE with Coomassie

staining. **(c)** Electrospray ionization mass spectrometry shows SnoopTag linked to SUMO-DogTag with loss of ammonia, following reaction with SnoopLigase. **(d)** SnoopLigase performed multiple rounds of product purification. Biotin-SnoopLigase was bound to streptavidin resin and used for conjugation of SUMO-DogTag and SnoopTagJr-AffiHER2 for 1 h at 4 °C. The resin was washed and the SnoopLigase reaction product eluted, before repeating the cycle. The amount of product formed relative to the first cycle was analyzed by SDS-PAGE with Coomassie staining (mean  $\pm$  1 SD, n = 9).

### **SnoopLigase-mediated cyclization made other enzymes thermoresilient.**

Many enzymes are active under a narrow range of conditions and are irreversibly inactivated outside those conditions.<sup>24</sup> Thermal resilience holds back the use of many enzymes in green chemical transformations.<sup>25</sup> Also, in agriculture enzymes are widely added to animal feed to enhance animal health and productivity. These enzymes suffer from substantial inactivation by the steam-treatment of feed to kill pathogens.<sup>26</sup> Phytase hydrolyzes the anti-nutrient phytic acid, increasing the digestibility of phytate-bound phosphate and reducing environmental phosphate pollution.<sup>26</sup> Inactivation of phytase during heat treatment of feed poses a major challenge.<sup>26</sup> Given the enormous diversity of enzymes available from nature, there is pressing need for generic approaches that can easily impart thermal resilience. Head-to-tail cyclization shows much potential to improve enzyme tolerance to harsh conditions, but with challenges including moderate yield of cyclization and insufficient increase of stability.<sup>27-28</sup>

To explore the stabilization potential of the SnoopLigase system, we cyclized the *Bacillus subtilis* phytase PhyC after genetically fusing SnoopTagJr at the N-terminus and DogTag at the C-terminus (Fig. 5A). SnoopTagJr-PhyC-DogTag cyclized rapidly and to high yield upon SnoopLigase addition, as visualized by an increased electrophoretic mobility of the cyclized form (Fig. 5B). Only a trace of higher order multimers from intermolecular reaction was seen (Fig. 5B). Isopeptide bond formation in SnoopTagJr-PhyC-DogTag was confirmed by mass spectrometry (Fig. S13). Similar efficient cyclization by SnoopLigase was seen for TEM-1  $\beta$ -lactamase (BLA), a favored model system for enzyme evolution (Fig. S14A,B).<sup>29</sup> PhyC is already moderately thermostable, surviving incubation at 55 °C. However, wild-type PhyC irreversibly aggregated at 75 °C, whereas SnoopLigase-cyclized SnoopTagJr-PhyC-DogTag remained soluble up to 100 °C (Fig. 5C). The improvement in PhyC solubility conferred by SnoopLigase cyclization was greater than that conferred by SpyTag/SpyCatcher (SpyRing-cyclization), tolerating even 1 hour at 100 °C (Fig. 5D,E).<sup>30-31</sup>

Wild-type BLA irreversibly aggregated at 37 °C, whereas SnoopLigase-cyclized SnoopTagJr-BLA-DogTag remained soluble after boiling, representing an increase in resilience of > 60 °C (Fig. 5F). To investigate the origin of the thermoresilience, we analyzed uncyclized SnoopTagJr-BLA-DogTag. Surprisingly, this construct was less aggregation-prone than wild-type BLA, but the stabilization was

less than with SnoopLigase cyclization (Fig. S14C). Also, the catalytically-inactive SnoopLigase EQ reduced the stabilization of SnoopTagJr-BLA-DogTag (Fig. S14C). Titration of BLA amount validated that these activity assays were sensitive to the amount of functional enzyme (Fig. S15).

To test whether catalytic activity was retained as well as solubility, we explored phytic acid hydrolysis by each PhyC construct. Indeed wild-type PhyC showed minimal activity after heating above 55 °C (Fig. 5G), whereas SnoopLigase-cyclized PhyC was almost fully active after 100 °C heating (Fig. 5H). Good retention of activity was also seen for SnoopLigase-cyclized BLA after 100 °C heating (Fig. S14D).

In the above tests, SnoopLigase was still present with cyclized enzyme. Using the solid-phase approach for conjugate purification, we tested the resilience of cyclized enzymes in the absence of SnoopLigase. Cyclized phytase after SnoopLigase depletion was much more resilient than linear phytase (in terms of both solubility and activity), but not quite as resilient as in the presence of SnoopLigase (Fig. 5, S16). For BLA, SnoopLigase depletion had only a marginal effect on solubility or activity after heating (Fig. S17). Overall, SnoopLigase-mediated cyclization shows strong potential as a simple method to achieve major improvements in enzyme thermoresilience.

**Figure 5**

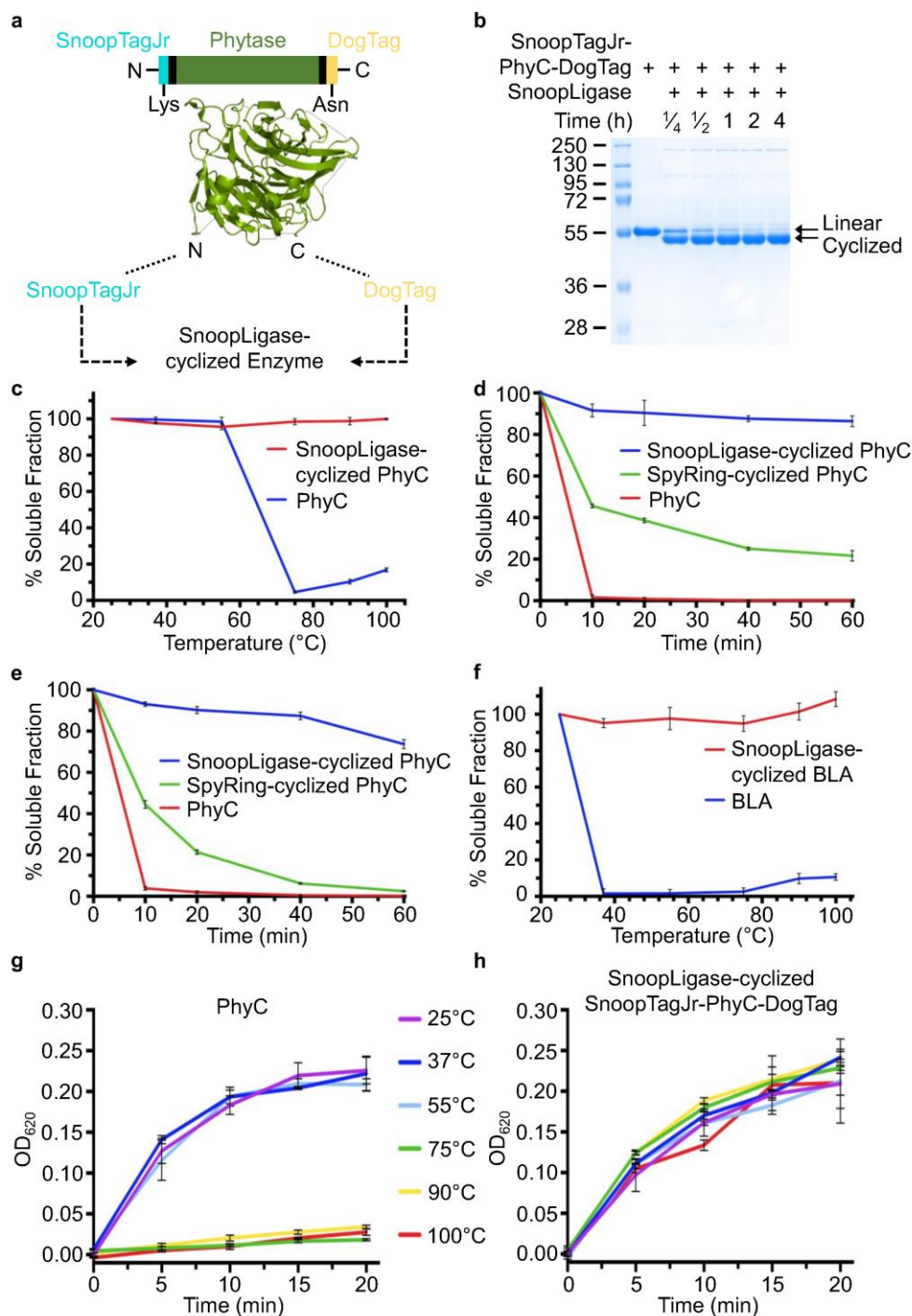


**Figure 5. SnoopLigase cyclization conferred thermal resilience to enzymes.** (a) Schematic of SnoopLigase enzyme cyclization. SnoopTagJr was positioned at the N-terminus and DogTag at the C-terminus of phytase, for SnoopLigase ligation, based on PDB 3AMR. (b) SnoopLigase efficiently cyclized SnoopTagJr-PhyC-DogTag. SnoopLigase and SnoopTagJr-PhyC-DogTag (10  $\mu$ M each) were incubated at 4 °C for 0.25-4 h, before SDS-PAGE with Coomassie staining. (c) SnoopLigase cyclization increased thermal resilience of phytase. PhyC or SnoopLigase-cyclized SnoopTagJr-PhyC-DogTag was incubated for 10 min at the indicated temperature, centrifuged to remove aggregates, and enzyme re-

remaining in the supernatant was quantified by SDS-PAGE with Coomassie staining. **(d)** PhyC, SpyRing-cyclized PhyC or SnoopLigase-cyclized SnoopTagJr-PhyC-DogTag at 10  $\mu$ M was incubated at 90 °C for the indicated times and the soluble fraction was measured as in (c). **(e)** PhyC variant resilience as in (d) at 100 °C. **(f)** As in (c) for BLA. **(g)** PhyC was incubated for 10 min at the indicated temperature and cooled to 25 °C, then used in colorimetric assays to quantify phosphate release from the hydrolysis of phytic acid. **(h)** SnoopLigase cyclization improved thermal resilience of PhyC activity. As for (g) with cyclized SnoopTagJr-PhyC-DogTag. All are mean of triplicate  $\pm$  1 SD.

## Conclusion

Here we have designed a catalyst for peptide-peptide ligation by isopeptide bond formation, able to conjugate to more than 95% completion under diverse mild conditions. Despite unpromising origins from the minimal activity of the initial split trio, we achieved a dramatically improved catalyst through our program of optimizing the splitting sites, proline-mediated loop rigidification, and computational stabilization. Lys/Asn transamidation has not been discovered as a modular way to join peptides in nature. Transglutaminases from various species do carry out Lys/Gln transamidation, via a thioester intermediate, but show low target specificity and also deamidate.<sup>32</sup> SnoopLigase exhibits much greater yield and tolerance of conditions than SpyLigase.<sup>8</sup> It remains to be tested how far the stabilization strategy here could enhance SpyLigase's applicability, to provide a pair of orthogonal ligases.<sup>12</sup>

*De novo* design of enzymes generally gives kinetics inferior to natural enzymes, including for the landmark computational design of a catalyst for Kemp elimination.<sup>33</sup> Given how SnoopLigase was designed, it is not surprising that the split protein forms a stable complex reforming the parent domain, so that SnoopLigase is majorly product-inhibited. The product inhibition prevents SnoopLigase from turning over substrate; however, turnover can be achieved by eluting the product and adding fresh substrate. This shows that SnoopLigase facilitates substrate conversion without itself undergoing a permanent chemical modification.

Due to product inhibition, SnoopLigase needs to be used at equimolar concentration as the substrates. However, for many applications the amount of enzyme is not the limiting factor – achieving efficient and specific coupling without extreme concentrations of substrate is more important. Indeed notable natural enzymes act as single turn-over catalysts, including in DNA repair, vitamin biosynthesis and CRISPR/Cas9.<sup>34-35</sup> For the widely-used catalyst sortase, a challenge has been the need for high concentrations of the oligoglycine partner ( $K_M$  140  $\mu$ M), despite a program of directed evolution.<sup>36</sup> Therefore, the oligoglycine partner is often desired at millimolar concentrations, which cannot be achieved for many proteins. Here we showed efficient SnoopLigase coupling with 2.5  $\mu$ M of DogTag or SnoopTagJr. In contrast to the recognition motifs of most conjugation methods (e.g. sortase, split

inteins, butelase, OaAEP1),<sup>3, 37-39</sup> SnoopTagJr and DogTag can be used as N- or C-terminal fusions, while DogTag also reacts efficiently when inserted within protein domains. This flexibility for tag insertion should extend the range of protein architectures achievable through peptide ligation.<sup>40-41</sup>

To address the challenge of conjugate purification, enzymes such as sortase have been coupled directly to cyanogen bromide-activated resin,<sup>23</sup> or conjugated with a bile acid for cyclodextrin-resin removal;<sup>42</sup> nevertheless, left-over substrate will remain. We made a virtue of the product inhibition of SnoopLigase, with solid-phase SnoopLigase attachment permitting elution of pure product after all starting material had been washed away. We report three different conditions for product elution and confirmed that elution conditions allowed retention of activity for fluorescent proteins, a ligand binding protein, and two enzymes.

We demonstrated the applicability of SnoopLigase cyclization to increase the thermal resilience of two different enzymes. Resilience is a key limiting factor for enzyme application. Resilience is usually enhanced by painstaking testing of hundreds to billions of enzyme variants.<sup>25, 29</sup>, so it is important to look for rapid and generic routes to achieve resilience. Enzyme cyclization by SnoopLigase was achieved to high yield in both cases. Cyclization has been a popular testing ground for bioconjugation approaches, including through carbodiimide chemistry,<sup>43</sup> split inteins,<sup>27</sup> sortase,<sup>37</sup> SpyTag/SpyCatcher,<sup>31</sup> butelase,<sup>38</sup> and OaAEP1,<sup>39</sup> providing increases in protease resistance, circulation time and thermodynamic stability.<sup>28</sup> However, the extent of thermoresilience achieved by SnoopLigase is surprising (with both enzymes resisting inactivation at 100 °C), surpassing previous approaches.<sup>44</sup> There is certainly more at play than the restricted conformational freedom of the enzyme termini after cyclization,<sup>30</sup> since depletion of SnoopLigase decreased the resilience of cyclized phytase. The increased resilience of BLA following fusion of SnoopTagJr and DogTag in the absence of cyclization also suggests an adventitious solubilizing effect of these sequences, which should be explored in future work.

Apart from the insights here for split protein re-design, SnoopLigase should provide many new opportunities for nanoassembly, including multispecific antibodies,<sup>9, 12, 45</sup> responsive biomaterials<sup>46-47</sup> and rapid vaccine construction.<sup>41, 48</sup>

## Experimental Section

**Cloning.** Plasmid constructs for protein expression were cloned using standard PCR procedures and Gibson isothermal assembly. Nucleotide sequences of gene inserts were validated by Sanger sequencing. Constructs for expression in *E. coli* contained an N-terminal His<sub>6</sub>-tag followed by a flexible GS-rich linker, except DogTag-mClover3 and DogTag-mKate2 contained a C-terminal His<sub>6</sub>-tag

preceded by a flexible GS-rich linker. Residue numbers of all RrgA-derived variants are based on the numbering of RrgA from Protein Data Bank ID code 2WW8.<sup>11</sup> pET28a-RrgA Ligase was derived by a deletion from pET28a-SnoopCatcher.<sup>12</sup> Sequential point mutations were introduced into pET28a-RrgA Ligase, finally giving pET28a-SnoopLigase (Fig. S1, GenBank accession no. MG867372). pET28a-SnoopLigase EQ was generated from pET28a-SnoopLigase, preventing catalysis by mutating Glu803 to Gln. pET28a-AviTag-SnoopLigase (Addgene plasmid ID 105626) contained an N-terminal AviTag for site-specific biotinylation.<sup>49</sup> pET28a-HaloTag7-SnoopLigase (Addgene plasmid ID 105627 and GenBank accession no. MG867371) was derived from pFC14A HaloTag CMV Flexi (Promega) and pET28a-SnoopLigase. pET28a-HaloTag7SS-SnoopTagJr was generated from pET28a-HaloTag7-SnoopLigase, with C61S and C261S mutations in HaloTag7.<sup>21</sup> pET28a-HaloTag7SS-DogTag inserted [HaloTag7SS with DogTag flanked by (GS)<sub>3</sub> linkers on either side, inserted between residues D139 and E140]<sup>20</sup> was derived from pET28a-HaloTag7SS-SnoopTagJr. pET28a-SnoopTagJr-MBP (Addgene plasmid ID 105628 and GenBank accession no. MG867374) was derived from pET28a-SnoopTag-MBP.<sup>12</sup> pET28a-MBP-DogTag inserted [MBP with DogTag flanked by (GS)<sub>3</sub> linkers on either side inserted between residues R317 and A319 (I318 deleted)]<sup>21</sup> was derived from pET28a-SnoopTagJr-MBP. pET28a-SnoopTagJr-AffiHER2 (encoding SnoopTagJr N-terminal to an affibody against HER2) and pET28a-AffiHER2-DogTag were derived from pET28a-SnoopTag-AffiHER2.<sup>48</sup> pET28a-SUMO-DogTag (Addgene plasmid ID 105629 and GenBank accession no. MG867376) was derived from pET28a-SUMO-KTag.<sup>8</sup> pET28a-SnoopTagJr-mEGFP was derived from pET28a-SnoopTag-mEGFP-SpyTag.<sup>12</sup> pET28a-DogTag-mClover3 was derived from pET28a-SpyTag002-mClover3.<sup>50</sup> mKate2<sup>51</sup> was a kind gift from Stephan Uphoff (University of Oxford) and was used to clone pET28a-DogTag-mKate2. pET28a-SnoopTagJr-BLA-DogTag (TEM-1  $\beta$ -lactamase flanked by SnoopTagJr and DogTag, GenBank accession no. MG867373) and variants thereof were derived from pET28a-BLA.<sup>31</sup> pET28a-SnoopTagJr-PhyC-DogTag (*B. subtilis* phytase flanked by SnoopTagJr and DogTag, GenBank accession no. MG867375) was derived from pET28a-PhyC.<sup>30</sup> pET28a-SpyTag-PhyC-SpyCatcher has been described.<sup>30</sup>

**Protein expression and purification.** Expression plasmids were transformed into *E. coli* BL21 (DE3)-RIPL (Agilent), except for SnoopTagJr-mEGFP which was transformed into *E. coli* C41<sup>52</sup>, a kind gift of Anthony Watts (University of Oxford). Individual colonies were grown in LB with 50  $\mu$ g/mL kanamycin for 16 h at 37 °C, 200 rpm. Starter cultures were diluted 1:100 in LB with 0.8% (w/v) glucose and 50  $\mu$ g/mL kanamycin, except for SnoopTagJr-BLA-DogTag, HaloTag7-SnoopLigase, HaloTag7SS-SnoopTagJr and HaloTag7SS-DogTag inserted, which were grown without glucose. Cultures were grown at 37 °C, 200 rpm until OD<sub>600</sub> 0.5. Cultures were induced with 0.42 mM IPTG and

grown for 4 h at 30 °C, 200 rpm, except for HaloTag7SS-SnoopTagJr and HaloTag7SS-DogTag-inserted, which were grown for 16 h at 20 °C, 200 rpm, before harvesting. Proteins were purified using standard Ni-NTA methods (Qiagen) and dialyzed three times. Buffers for dialysis were TB pH 8.0 (50 mM Tris base adjusted to pH 8.0 with boric acid) for AviTag-SnoopLigase, SnoopTagJr-MBP and MBP-DogTag-inserted; TB pH 7.4 (50 mM Tris base adjusted to pH 7.4 with boric acid) for HaloTag7SS-SnoopTagJr; 50 mM sodium borate pH 10.0 for RrgA Ligase (and point mutants), SnoopLigase, SnoopTag-AffiHER2, SnoopTagJr-AffiHER2 and SUMO-DogTag; PBS (137 mM NaCl, 2.7 mM KCl, 10 mM Na<sub>2</sub>HPO<sub>4</sub>, 2 mM KH<sub>2</sub>PO<sub>4</sub>, pH 7.4) for BLA-containing constructs, SnoopTagJr-mEGFP, DogTag-mClover3 and DogTag-mKate2; 50 mM Tris•HCl pH 8.0 for HaloTag7SS-DogTag inserted; 50 mM Tris•HCl pH 7.0, 2 mM CaCl<sub>2</sub> for PhyC-containing constructs. Biotinylation of AviTag-SnoopLigase was performed as described previously.<sup>49</sup> His-tagged SUMO protease Ulp1 in pOPINE has been described.<sup>53</sup> To determine protein concentrations, OD<sub>280</sub> was measured using an ND-1000 Nanodrop (NanoDrop) with the extinction coefficient predicted by ExPASy ProtParam.

**SnoopLigase reactions.** In standard conditions to assess the formation of the isopeptide bond between SnoopTagJr and DogTag, proteins were incubated at 10 μM each in TB pH 7.25 + 15% (v/v) glycerol at 4 °C for 2 h, unless indicated otherwise. To measure pH-dependence, reactions were run in standard conditions, but in 50 mM Tris base adjusted to the indicated pH with boric acid. To measure temperature-dependence, reactions were run in standard conditions from 4-37 °C. To measure NaCl-dependence, reactions were run in standard conditions ± 137 mM NaCl. To measure detergent-dependence, reactions were run in standard conditions with 0.5, 1 or 2% Tween 20 (v/v), Triton X-100 (v/v) or SDS (w/v). To measure glycerol-dependence, reactions were run in standard conditions with 0-40% (v/v) glycerol. To measure reducing agent-dependence, reactions were run in standard conditions with 100 mM 2-mercaptoethanol (βME) or 20 mM dithiothreitol (DTT). To terminate the reaction, 6× SDS loading buffer [0.23 M Tris•HCl, pH 6.8, 24% (v/v) glycerol, 120 μM bromophenol blue, 0.23 M SDS] was added to a final concentration of 1×.

**Bioinformatic and computational design of SnoopLigase mutations.** To identify residues for proline substitution, Ramachandran analysis of amino acid residues in RrgA (PDB code 2WW8) was performed using MolProbity.<sup>54</sup> Loop residues with  $\phi$ -angles of -70° to -50° were considered for proline substitution. Homologous sequences for RrgA residues 734-860 were collected using Position-Specific Iterative Basic Local Alignment Search Tool (PSI-BLAST)<sup>55</sup> and aligned using Multiple Sequence Comparison by Log-Expectation (MUSCLE).<sup>56</sup> Cluster Database at High Identity with Tolerance (CD-

HIT)<sup>57</sup> was used to minimize sequence redundancy and tune the size of the dataset before PROSS analysis.<sup>17</sup> The output amino acid substitutions were reviewed manually in PyMOL (DeLano Scientific).

**Rosetta modeling of RrgA mutations.** Modeling of mutations in RrgA was performed using Rosetta3.<sup>18</sup> The crystal structure of RrgA (PDB code 2WW8) residues 734-860 with G842T, N847D and D848G mutations was relaxed and the pmut\_scan protocol was used to calculate Rosetta Energy units (R.E.U.) for mutants.

**Purification of SnoopLigase reaction product by glycine elution.** SUMO-DogTag, SnoopTagJr-AffiHER2 and biotin-SnoopLigase at 10  $\mu$ M each in TB pH 7.25 with 15% (v/v) glycerol in a total volume of 200  $\mu$ L were incubated for 20 h at 4 °C. To capture SnoopLigase, 25  $\mu$ L washed and equilibrated HiCap Streptavidin Agarose (Thermo Fisher) was added and samples were incubated for 30 min at 25 °C on a tube rotor. The resin was collected in a 1 mL poly-prep column (Bio-Rad) and spun for 1 min at 300 g at 4 °C. All subsequent steps were performed at 4 °C. After washing the resin twice with 125  $\mu$ L 50 mM glycine pH 3.0 with 300 mM NaCl and three times with 125  $\mu$ L 50 mM glycine pH 3.0, one extra spin for 1 min at 500 g ensured the removal of excess liquid from the resin. To elute the SnoopLigase reaction product, the resin was incubated with 25  $\mu$ L antibody elution buffer (50 mM glycine pH 2.0) for 1 min, before spinning the eluate into a tube containing 2.5  $\mu$ L 1 M Tris•HCl pH 9.5 for 1 min at 300 g, to neutralize the eluate. The elution was repeated twice more.

**Purification of SnoopLigase reaction product by imidazole elution.** For capture with HaloLink Resin, SUMO-DogTag, SnoopTagJr-AffiHER2 and HaloTag7-SnoopLigase at 15  $\mu$ M each in TB pH 7.25 with 15% (v/v) glycerol in a total volume of 200  $\mu$ L were incubated for 24 h at 4 °C. Imidazole was added to a final concentration of 0.5 M and Tween 20 to a final concentration of 0.01% (v/v). To capture HaloTag7-SnoopLigase, 20  $\mu$ L washed and equilibrated HaloLink resin (Promega) was added and samples were incubated for 1 h at 25 °C on a tube rotor. The resin was collected in a buffer-equilibrated 1 mL poly-prep column (Bio-Rad) and spun for 1 min at 300 g at 25 °C. After washing the resin five times with 150  $\mu$ L Tris-phosphate pH 7.0 (25 mM phosphoric acid adjusted to pH 7.0 with Tris base) with 500 mM imidazole pH 7.0 (adjusted with HCl) and 0.01% (v/v) Tween 20 at 25 °C, one extra spin for 1 min at 500 g and 25 °C ensured the removal of excess liquid from the resin. To elute the reaction product, the resin was incubated with 20  $\mu$ L Tris-phosphate with 2 M imidazole pH 7.0 and 0.01% (v/v) Tween 20 for 5 min at 25 °C on a Thermomixer comfort (Eppendorf) at 800 rpm, before spinning the eluate into a tube for 1 min at 300 g, 25 °C. The elution was repeated twice more.

For capture with streptavidin resin, enzymes flanked by SnoopTagJr and DogTag were incubated with biotin-SnoopLigase at 10  $\mu$ M in TB pH 7.25 + 15% (v/v) glycerol at 4 °C for 16 h. Cyclization reactions of PhyC were supplemented to a final concentration of 2 mM CaCl<sub>2</sub>. Following cyclization, 10  $\mu$ L washed and equilibrated streptavidin agarose was added per 100  $\mu$ L reaction and incubated at 25 °C for 30 min on a tube rotor. 1 mL poly-prep columns were prepared by washing with 1 M imidazole + 0.01% Tween-20. The reaction was loaded on the columns and spun for 1 min at 300 g, followed by 5 washes with 5 resin volumes of 0.5 M imidazole + 0.01% (v/v) Tween 20 in 250 mM Tris-phosphate pH 7.0 at 25 °C. Columns were spun for 1 min at 500 g. To elute cyclized enzyme, the poly-prep columns were capped before the addition of 1 resin volume of 2.5 M imidazole + 0.01% (v/v) Tween 20 in 250 mM Tris-phosphate pH 7.0. The columns were incubated for 2 min on a Thermomixer at 800 rpm, 25 °C. This was repeated 3 more times for a final elution volume of 4 resin volumes. All wash and elution buffers were supplemented to a final concentration of 2 mM CaCl<sub>2</sub> for phytase elution. The eluted enzymes were dialyzed into their optimum buffer and concentrated in 5 kDa molecular weight cut-off filters (Vivaspin 500, GE Healthcare).

**SnoopLigase removal by peptide elution.** SUMO-DogTag, SnoopTagJr-AffiHER2 and biotin-SnoopLigase at 10  $\mu$ M each in TB pH 7.25 with 15% (v/v) glycerol in a total volume of 150  $\mu$ L were incubated for 16 h at 4 °C. Tween 20 was added to a final concentration of 0.01% (v/v). To capture biotin-SnoopLigase, 15  $\mu$ L washed and equilibrated HiCap Streptavidin Agarose (Thermo Fisher) was added and the sample incubated for 30 min at 25 °C on a tube rotor. The resin was collected in a PCR tube (StarLab) and spun for 1 min at 300 g at 25 °C, followed by five washes with 75  $\mu$ L Tris-phosphate pH 7.0 with 0.01% (v/v) Tween 20. 30  $\mu$ L DogTag:SnoopTagJr in TB pH 7.5 with 0.01% (v/v) Tween 20 was added and the sample incubated for 4 h at 37 °C at 800 rpm on a Thermomixer. The sample was centrifuged for 1 min at 16,900 g and the supernatant collected.

For cyclized enzyme purification, enzymes flanked by SnoopTagJr and DogTag were incubated with biotin-SnoopLigase (each 10  $\mu$ M) for 16 h at 4 °C in TB pH 7.25 + 15% (v/v) glycerol. 10  $\mu$ L washed and equilibrated HiCap Streptavidin Agarose (Thermo Fisher) was added per 100  $\mu$ L cyclization reaction and incubated for 30 min at 25 °C on a tube rotor. The reaction was spun down for 1 min at 6,000 g at 25 °C, followed by five washes with five resin volumes of Tris-phosphate pH 7.0 + 0.01% (v/v) Tween 20. 2  $\mu$ L 100  $\mu$ M DogTag:SnoopTagJr was added per  $\mu$ L resin in TB pH 7.5 + 0.01% (v/v) Tween 20 and incubated for 4 h at 37 °C, 800 rpm on a Thermomixer. The sample was centrifuged for 1 min at 16,900 g and the supernatant collected.

**Analyzing the effect of imidazole on model protein function.** SnoopTagJr-mEGFP, DogTag-mKate2 or HaloTag7SS-SnoopTagJr (25  $\mu$ M each) were incubated in Tris-phosphate pH 7.0 (25 mM phosphoric acid adjusted to pH 7.0 with Tris base) with or without 2 M imidazole pH 7.0 (adjusted with HCl) for 10 min at 25  $^{\circ}$ C, followed by dialysis into 50 mM Tris•HCl pH 8.0. 96-well clear flat-bottom polystyrene plates (Greiner) were blocked with 45  $\mu$ L 50 mM Tris•HCl pH 8.0 containing 1% (w/v) BSA (bovine serum albumin, Sigma-Aldrich) in each well at 25  $^{\circ}$ C for 10 min before addition of fluorescent proteins at 0.5  $\mu$ M final concentration. Fluorescence was recorded at  $\lambda_{\text{ex}} = 485$  nm,  $\lambda_{\text{em}} = 538$  nm for SnoopTagJr-mEGFP and  $\lambda_{\text{ex}} = 544$  nm,  $\lambda_{\text{em}} = 612$  nm for DogTag-mKate2 using a SpectraMax M3 microplate reader (Molecular Devices). To measure HaloTag7SS-SnoopTagJr activity, the dialyzed protein at 5  $\mu$ M was incubated with 2  $\mu$ L washed and equilibrated HaloLink resin (Promega) in a total volume of 20  $\mu$ L for 5 min at 25  $^{\circ}$ C on a tube rotor. Samples were centrifuged for 30 s at 16,900 g at 25  $^{\circ}$ C and 10  $\mu$ L of supernatant was collected. The amount of HaloTag7SS-SnoopTagJr coupled to the resin was determined by comparing the amount of protein in the supernatant to the input, using SDS-PAGE with Coomassie staining and densitometry.

**Production of DogTag:SnoopTagJr competitor.** 4 mL HaloTag7-SnoopLigase at 20  $\mu$ M in 50 mM TB pH 7.25 with 0.01% (v/v) Tween 20 was incubated with 500  $\mu$ L packed HaloLink resin (Promega) for 2 h at 25  $^{\circ}$ C on a tube rotor. The sample was split into five buffer-equilibrated 1 mL poly-prep columns (Bio-Rad) and spun for 1 min at 300 g at 25  $^{\circ}$ C. Each resin sample was washed twice with 500  $\mu$ L 50 mM TB pH 7.25 with 0.01% (v/v) Tween 20. Columns were capped and 200  $\mu$ L reaction buffer [50  $\mu$ M SUMO-DogTag and 75  $\mu$ M SnoopTagJr peptide in TB pH 7.25 with 15% (v/v) glycerol] was added to each column. SnoopTagJr peptide had the sequence GKLGSIEFIKVNKGY and was solid-phase synthesized by Activotec at >95% purity. After incubation for 4 h at 25  $^{\circ}$ C at 300 rpm on a Thermomixer, samples were spun for 1 min at 300 g at 25  $^{\circ}$ C and each resin sample was washed five times with 500  $\mu$ L Tris-phosphate pH 7.0 with 0.5 M imidazole and 0.01% (v/v) Tween 20. To elute the SnoopLigase reaction product, each resin sample was incubated with 100  $\mu$ L Tris-phosphate with 2.5 M imidazole pH 7.0 and 0.01% (v/v) Tween 20 for 2 min at 25  $^{\circ}$ C on a Thermomixer at 800 rpm, before spinning the eluate into a tube for 1 min at 300 g, at 25  $^{\circ}$ C. The elution was repeated twice more and each resin washed twice with 500  $\mu$ L TB pH 7.25 with 0.01% (v/v) Tween 20. To start the next reaction cycle, fresh reaction mix was added to the resin and the reaction and purification procedure repeated. Six reaction cycles were performed in total. All elutions were pooled, dialyzed into TB pH 7.5 and SUMO-DogTag:SnoopTagJr was concentrated to 118  $\mu$ M using a 10 kDa MWCO spin filter (Sartorius). SUMO protease Ulp1 was added at 1:50 molar ratio to a final concentration of 2.4  $\mu$ M, followed by 45 min incubation at 25  $^{\circ}$ C. After reaction, Tween 20 was added to a final concentration of 0.01% (v/v). To

deplete His-tagged proteins (SUMO and Ulp1), 600  $\mu\text{L}$  sample was incubated with 150  $\mu\text{L}$  packed Ni-NTA agarose (Qiagen) for 1 h at 25  $^{\circ}\text{C}$  on a tube rotor, the sample centrifuged for 1 min at 16,900 g at 25  $^{\circ}\text{C}$ , and the supernatant containing the DogTag:SnoopTagJr conjugate was collected. The concentration was calculated using the  $\text{OD}_{280}$  extinction coefficient from ExPASy ProtParam.

**SnoopLigase  $K_M$  determination.** To determine the  $K_M$  for SnoopTagJr-AffiHER2, SnoopLigase at 5  $\mu\text{M}$  and SUMO-DogTag at 40  $\mu\text{M}$  were incubated with 3.75-60  $\mu\text{M}$  SnoopTagJr-AffiHER2 in TB pH 7.25 + 15% (v/v) glycerol at 4  $^{\circ}\text{C}$  for 7.5 min. To terminate the reaction, 6 $\times$  SDS loading buffer was added to a final concentration of 1 $\times$ . The  $K_M$  of SUMO-DogTag was determined the same way but with SnoopTagJr-AffiHER2 at 40  $\mu\text{M}$  and SUMO-DogTag at 3.75-60  $\mu\text{M}$ . To quantify the amount of product formed, a product standard for gel densitometry was generated by conjugating 10  $\mu\text{M}$  SnoopTagJr-AffiHER2 to SUMO-DogTag at 20  $\mu\text{M}$  using 20  $\mu\text{M}$  SnoopLigase under standard reaction conditions for 48 h. The molar ratios ensured > 95% conjugation of SnoopTagJr-AffiHER2, such that the concentration of SnoopTagJr-AffiHER2:SUMO-DogTag was considered 10  $\mu\text{M}$ . Samples were analyzed by SDS-PAGE with Coomassie staining, followed by densitometry. Reaction rates were fit to the Michaelis-Menten equation to determine  $K_M$  values.

**Lyophilization stability.** 30  $\mu\text{L}$  aliquots of SnoopLigase at 10  $\mu\text{M}$  in TB pH 7.25 were prepared in 100  $\mu\text{L}$  thin-wall PCR tubes (StarLab). Samples were flash-frozen in a dry ice-ethanol bath for 10 min and lyophilized using a BenchTop 2K freeze-dryer (VirTis) for 48 h at 0.14 mbar and  $-72.5^{\circ}\text{C}$ . Lyophilized samples were stored at 37  $^{\circ}\text{C}$  for the indicated time in a glass scintillation vial sealed with Parafilm (Sigma-Aldrich) on a bed of Drierite (Sigma-Aldrich) to minimize sample hydration. Samples were reconstituted in reaction buffer and the reaction of SnoopTagJr-AffiHER2 and SUMO-DogTag was performed for 2 h at 4  $^{\circ}\text{C}$ , followed by SDS-PAGE, Coomassie staining and densitometry.

**Size exclusion chromatography (SEC) of a SnoopLigase reaction.** AffiHER2-DogTag, SnoopTagJr-MBP and biotin-SnoopLigase at 50  $\mu\text{M}$  each in TB pH 7.25 with 15% (v/v) glycerol in a total volume of 1000  $\mu\text{L}$  were incubated for 24 h at 4  $^{\circ}\text{C}$ . Imidazole pH 7.0 was added to a final concentration of 0.5 M and Tween 20 to a final concentration of 0.01% (v/v). To capture biotin-SnoopLigase, 300  $\mu\text{L}$  washed and equilibrated HiCap Streptavidin Agarose (Thermo Fisher) was added and samples were incubated for 30 min at 25  $^{\circ}\text{C}$  on a tube rotor. The sample was collected in three buffer-equilibrated 1 mL poly-prep columns (Bio-Rad) and spun for 1 min at 300 g at 25  $^{\circ}\text{C}$ . After washing the resin five times with 500  $\mu\text{L}$  Tris-phosphate pH 7.0 (25 mM phosphoric acid adjusted to pH 7.0 with Tris base) with 500 mM imidazole pH 7.0 (adjusted with HCl) and 0.01% Tween 20 (v/v) at 25  $^{\circ}\text{C}$ , one extra spin for 1 min at

500 g at 25 °C ensured the removal of excess liquid from the resin. To elute the SnoopLigase reaction product, the resin was incubated with 100 µL Tris-phosphate with 2 M imidazole pH 7.0 and 0.01% (v/v) Tween 20 for 5 min at 25 °C on a Thermomixer at 300 rpm, before spinning the eluate into a tube for 1 min at 300 g, at 25 °C. The elution was repeated twice more. 500 µL of the purified elution, a reaction sample without product purification, 50 µM biotin-SnoopLigase, 50 µM AffiHER2-DogTag or 50 µM SnoopTagJr-MBP were dialyzed into 50 mM sodium borate pH 10.0. 200 µL of the samples were applied to a previously equilibrated Superdex 75 increase 10/300 GL (GE Healthcare) on a fast protein liquid chromatography (FPLC) system Purifier 10 (GE Healthcare) at 4 °C, using 50 mM sodium borate pH 10.0 as mobile-phase column buffer.

**Solid-phase ligation reaction cycles.** Biotin-SnoopLigase at 50 µM in TB pH 8.0 was coupled to 10 µL washed and equilibrated HiCap Streptavidin Agarose in a total volume of 50 µL for 30 min at 25 °C on a tube rotor. The resin was collected in a 1 mL poly-prep column and spun for 1 min at 300 g, followed by five washes with 100 µL TB pH 8.0 at 25 °C. The reaction was started by addition of 50 µL reaction mix [50 µM SUMO-DogTag and 50 µM SnoopTagJr-AffiHER2 in TB pH 7.25 with 15% (v/v) glycerol] and the sample was incubated for 1 h at 4 °C on a Thermomixer at 800 rpm. The reaction mixture was spun for 1 min at 300 g and the resin washed twice with 50 µL 50 mM glycine pH 3.0 with 300 mM NaCl and three times with 50 µL 50 mM glycine pH 3.0, all at 4 °C. One extra spin for 1 min at 500 g at 4 °C ensured the removal of excess liquid from the resin. To elute the SnoopLigase reaction product, the resin was incubated with 10 µL antibody elution buffer for 1 min, before spinning the eluate into a tube containing 1 µL 1 M Tris•HCl pH 9.5 for 1 min at 300 g. The elution was repeated twice more. The resin was washed twice with 100 µL antibody elution buffer and twice with 100 µL TB pH 7.25 to ensure complete removal of residual reaction product, all at 4 °C. To start the next reaction cycle, fresh reaction mix was added to the resin and the reaction and purification procedure repeated. Eight reaction cycles were performed in total.

**SnoopLigase thermostability.** SnoopLigase at 12.5 µM in TB pH 7.25 with 15% (v/v) glycerol was incubated at the indicated temperature for 15 min on a C1000 thermal cycler (Bio-Rad) and cooled to 4 °C for 5 min. Heat-treated SnoopLigase was used for ligation of SnoopTagJr-AffiHER2 and SUMO-DogTag as described above.

**Enzyme cyclization by SnoopLigase.** To cyclize enzymes flanked by SnoopTagJr and DogTag, 10 µM enzyme construct and 10 µM SnoopLigase were incubated in TB pH 7.25 + 15% (v/v) glycerol at 4 °C for 16 h. Cyclization reactions of SnoopTagJr-PhyC-DogTag for thermal resilience activity assays were

supplemented to a final concentration of 2 mM CaCl<sub>2</sub>. For the cyclization time-course, reaction was terminated by adding SDS loading buffer as above.

**Temperature-dependent solubility assays.** For BLA constructs, 20 µL 10 µM enzyme in PBS with 100 mM dithiothreitol was incubated at 10, 25, 37, 55, 75, 90 or 100 °C for 10 min, then cooled to 10 °C (ramp rate 3 °C/s) on a C1000 thermal cycler. For PhyC constructs, 20 µL 10 µM enzyme in 50 mM Tris•HCl pH 7.0 with 2 mM CaCl<sub>2</sub> was incubated in the same manner. For time-course assays, 20 µL 10 µM PhyC construct in 50 mM Tris•HCl pH 7.0, with 2 mM CaCl<sub>2</sub> was incubated at 90 or 100 °C for 10, 20, 40 or 60 min, then cooled to 10 °C (ramp rate 3 °C/s) on a C1000 thermal cycler. Following heating, aggregated proteins were pelleted by centrifugation at 4 °C, 16,900 g for 30 min. The supernatant was run on SDS-PAGE. The samples held at 10 °C were defined as 100% soluble.

**BLA thermal resilience activity assays.** 96-well clear flat-bottom polystyrene plates (Greiner) were blocked with 200 µL PBS, 3% (w/v) BSA (bovine serum albumin, Sigma-Aldrich) in each well at 37 °C for a minimum of 2 h. Blocked plates were washed twice with 0.1 M NaH<sub>2</sub>PO<sub>4</sub> pH 7.0 with 1 mM ethylenediaminetetraacetic acid (EDTA). 20 µL 25 µM BLA construct was incubated at 10, 25, 37, 55, 75, 90 or 100 °C for 10 min, then cooled to 10 °C (ramp rate 3 °C/s) on a C1000 thermal cycler (Bio-Rad). The samples were diluted to a final concentration of 62.5 nM using 0.1 M NaH<sub>2</sub>PO<sub>4</sub> pH 7.0 with 1 mM EDTA. Nitrocefin (Merck) substrate solution was prepared to 105 µM through the addition of 0.1 M NaH<sub>2</sub>PO<sub>4</sub> pH 7.0 with 1 mM EDTA. The diluted BLA constructs were reacted at a final concentration of 3 nM with 100 µM nitrocefin. The SpectraMax M3 microplate reader (Molecular Devices) was used to measure OD<sub>486</sub> every 15 s for 10 min at 20 °C, with automatic mixing for 3 s between measurements. Blanks consisted of all components except the enzyme.

**PhyC thermal resilience activity assays.** 96-well clear flat-bottom polystyrene plates (Greiner) were blocked with 200 µL 50 mM Tris•HCl pH 7.0 with 2 mM CaCl<sub>2</sub> and 3% (w/v) BSA at 37 °C for 2 h. Blocked plates were washed twice with 50 mM Tris•HCl pH 7.0 with 2 mM CaCl<sub>2</sub> and 10% (v/v) glycerol. 10 µM enzyme was incubated at 25, 37, 55, 75, 90 and 100 °C for 10 min, then cooled to 10 °C (ramp rate 3 °C/s) on a C1000 thermal cycler (Bio-Rad). The samples were diluted to 375 nM using 50 mM Tris•HCl pH 7.0 with 2 mM CaCl<sub>2</sub>. 25 µM phytic acid sodium salt (Sigma-Aldrich) substrate solution was prepared using 50 mM Tris•HCl pH 7.0 with 2 mM CaCl<sub>2</sub>. In the final reaction, 75 nM phytase construct reacted with 20 µM phytic acid at 50 °C, 350 rpm on a Thermomixer. Reactions were set up such that all time-points finished at the same time. 100 µL Biomol Green (Enzo Life Sciences) was added immediately to each well and the plate was incubated at 25 °C for 25 min for color development. The

SpectraMax M3 microplate reader was used to measure OD<sub>620</sub> at 20 °C. Blanks consisted of all components except the enzyme. Some error bars are too small to be visible.

**SDS-PAGE and reaction quantification.** Samples were mixed with 6× SDS loading buffer to a final concentration of 1×. For all samples containing BLA constructs, dithiothreitol was added to a final concentration of 100 mM. For all samples containing PhyC constructs, EDTA was added to a final concentration of 100 mM. Samples were heated for 3 min at 99 °C and allowed to cool to 25 °C for 10 min before loading. SDS-PAGE was performed at 200 V in 25 mM Tris•HCl, 192 mM glycine, 0.1% (w/v) SDS. Gels were stained with InstantBlue Coomassie stain (Expedeon), destained with MilliQ water and imaged using a ChemiDoc XRS imager with ImageLab software (Bio-Rad). ImageLab was also used for band quantification. “% Product formed” was calculated from band intensities as  $100 \times [\text{product}] / ([\text{product}] + [\text{DogTag substrate}] + [\text{SnoopTagJr substrate}])$ . Relative product formed was calculated as percentage of product formed under that condition divided by the percentage of product formed from the control (Fig. 3A pH 7.25; Fig. 3B 4 °C, Fig. 3D no detergent, Fig. 3E 0% glycerol, Fig. 3F, 4 °C, Fig. 4D cycle 1, Fig. S8A non-lyophilized, Fig. S8B no reducing agent). “% partner reacted” was calculated from band intensities as  $100 \times (1 - [\text{substrate after reaction}] / [\text{substrate before reaction}])$ .

**Mass spectrometry.** SUMO-DogTag at 75 μM and a SnoopTag-containing solid-phase synthesized peptide (GKLGDIIEFIKVNKGY, Insight Biotechnology at 95% purity) at 300 μM were incubated with 75 μM biotin-SnoopLigase in TB pH 7.25 and 15% (v/v) glycerol in a total volume of 200 μL for 36 h at 4 °C. The reaction product was purified with glycine elution as above, but with 100 μL HiCap Streptavidin Agarose and 500 μL wash buffer. Analysis of this reaction or SUMO-DogTag alone was performed using a Micromass LCT time-of-flight electrospray ionization mass spectrometer (Micromass). The molecular mass profile was created from the m/z spectrum using V4.00.00 software (Waters) with a maximum entropy algorithm. The observed mass of SUMO-DogTag was consistent with the mass predicted by ExPASy ProtParam, based on the amino acid sequence without N-terminal fMet and with one acetylation from *E. coli* expression. The increase in mass after reaction of SUMO-DogTag with peptide was predicted from the mass of the peptide calculated by ExPASy ProtParam and loss of ammonia (17.0 Da) during isopeptide bond formation. SnoopTagJr-PhyC-DogTag or cyclized SnoopTagJr-PhyC-DogTag following SnoopLigase removal was dialysed into 10 mM ammonium acetate + 2 mM CaCl<sub>2</sub>. Mass spectrometry and analysis was performed as above.

## ASSOCIATED CONTENT

### Supporting Information

The Supporting Information is available free of charge on the ACS Publications website at DOI:

<<please fill in>>.

Figures S1-S17 (PDF)

## Acknowledgements

Funding for C.M.B. was provided by the Engineering and Physical Sciences Research Council (EPSRC) and Corpus Christi College Oxford. Funding for J.X.J. was provided by the Biotechnology and Biological Sciences Research Council (BBSRC) and AB Vista. We thank Matteo Ferla (University of Oxford) for bioinformatic assistance.

## Author contributions:

|| C.M.B. and J.X.J. contributed equally.

## Additional information

Competing financial interests: M.H. and C.M.B. are authors on a patent application covering peptide-peptide ligation: UK Intellectual Property Office 1705750.6.

## References

1. Liu, Z.; Lavis, L. D.; Betzig, E. *Mol. Cell* **2015**, *58* (4), 644-659.
2. McCluskey, A. J.; Collier, R. J. *Mol. Cancer Ther.* **2013**, *12* (10), 2273-2281.
3. Stephanopoulos, N.; Francis, M. B. *Nat. Chem. Biol.* **2011**, *7* (12), 876-884.
4. Liu, Z.; Chen, X. *Chem. Soc. Rev.* **2016**, *45* (5), 1432-1456.
5. Wood, D. W. *Curr. Opin. Struct. Biol.* **2014**, *26C*, 54-61.
6. Chin, J. W. *Annu. Rev. Biochem.* **2014**, *83*, 379-408.
7. Kang, H. J.; Baker, E. N. *Trends Biochem. Sci.* **2011**, *36* (4), 229-237.
8. Fierer, J. O.; Veggiani, G.; Howarth, M. *Proc. Natl. Acad. Sci. U. S. A.* **2014**, *111* (13), E1176-1181.
9. Siegmund, V.; Piater, B.; Zakeri, B.; Eichhorn, T.; Fischer, F.; Deutsch, C.; Becker, S.; Toleikis, L.; Hock, B.; Betz, U. A.; Kolmar, H. *Sci. Rep.* **2016**, *6*, 39291.
10. Charville, H.; Jackson, D. A.; Hodges, G.; Whiting, A.; Wilson, M. R. *Eur. J. Org. Chem.* **2011**, (30), 5981-5990.
11. Izore, T.; Contreras-Martel, C.; El Mortaji, L.; Manzano, C.; Terrasse, R.; Vernet, T.; Di Guilmi, A. M.; Dessen, A. *Structure* **2010**, *18* (1), 106-115.
12. Veggiani, G.; Nakamura, T.; Brenner, M. D.; Gayet, R. V.; Yan, J.; Robinson, C. V.; Howarth, M. *Proc. Natl. Acad. Sci. U. S. A.* **2016**, *113* (5), 1202-1207.
13. Shekhawat, S. S.; Ghosh, I. *Curr. Opin. Chem. Biol.* **2011**, *15* (6), 789-797.
14. Papaleo, E.; Saladino, G.; Lambroughi, M.; Lindorff-Larsen, K.; Gervasio, F. L.; Nussinov, R. *Chem. Rev.* **2016**, *116* (11), 6391-6423.
15. Trevino, S. R.; Schaefer, S.; Scholtz, J. M.; Pace, C. N. *J. Mol. Biol.* **2007**, *373* (1), 211-218.
16. Fu, H.; Grimsley, G. R.; Razvi, A.; Scholtz, J. M.; Pace, C. N. *Proteins* **2009**, *77* (3), 491-498.

17. Goldenzweig, A.; Goldsmith, M.; Hill, S. E.; Gertman, O.; Laurino, P.; Ashani, Y.; Dym, O.; Unger, T.; Albeck, S.; Prilusky, J.; Lieberman, R. L.; Aharoni, A.; Silman, I.; Sussman, J. L.; Tawfik, D. S.; Fleishman, S. J. *Mol. Cell* **2016**, *63* (2), 337-346.
18. Leaver-Fay, A.; Tyka, M.; Lewis, S. M.; Lange, O. F.; Thompson, J.; Jacak, R.; Kaufman, K.; Renfrew, P. D.; Smith, C. A.; Sheffler, W.; Davis, I. W.; Cooper, S.; Treuille, A.; Mandell, D. J.; Richter, F.; Ban, Y. E.; Fleishman, S. J.; Corn, J. E.; Kim, D. E.; Lyskov, S.; Berrondo, M.; Mentzer, S.; Popovic, Z.; Havranek, J. J.; Karanicolas, J.; Das, R.; Meiler, J.; Kortemme, T.; Gray, J. J.; Kuhlman, B.; Baker, D.; Bradley, P. *Methods Enzymol.* **2011**, *487*, 545-574.
19. Wikman, M.; Steffen, A. C.; Gunneriusson, E.; Tolmachev, V.; Adams, G. P.; Carlsson, J.; Stahl, S. *Protein Eng. Des. Sel.* **2004**, *17* (5), 455-462.
20. Ishikawa, H.; Meng, F.; Kondo, N.; Iwamoto, A.; Matsuda, Z. *Protein Eng. Des. Sel.* **2012**, *25* (12), 813-820.
21. Ke, N.; Landgraf, D.; Paulsson, J.; Berkmen, M. *J. Bacteriol.* **2016**, *198* (7), 1035-1043.
22. Moser, A. C.; Hage, D. S. *Bioanalysis* **2010**, *2* (4), 769-790.
23. Witte, M. D.; Wu, T.; Guimaraes, C. P.; Theile, C. S.; Blom, A. E.; Ingram, J. R.; Li, Z.; Kundrat, L.; Goldberg, S. D.; Ploegh, H. L. *Nat. Protoc.* **2015**, *10* (3), 508-516.
24. Sanchez-Ruiz, J. M. *Biophys. Chem.* **2010**, *148* (1-3), 1-15.
25. Stepankova, V.; Bidmanova, S.; Koudelakova, T.; Prokop, Z.; Chaloupkova, R.; Damborsky, J. *ACS Catalysis* **2013**, *3* (12), 2823-2836.
26. Lei, X. G.; Weaver, J. D.; Mullaney, E.; Ullah, A. H.; Azain, M. J. *Annu. Rev. Anim. Biosci.* **2013**, *1*, 283-309.
27. Iwai, H.; Pluckthun, A. *FEBS Lett.* **1999**, *459* (2), 166-172.
28. Borra, R.; Camarero, J. A. *Biopolymers* **2013**, *100* (5), 502-509.
29. Bershtein, S.; Goldin, K.; Tawfik, D. S. *J. Mol. Biol.* **2008**, *379* (5), 1029-1044.
30. Schoene, C.; Bennett, S. P.; Howarth, M. *Sci. Rep.* **2016**, *6*, 21151.
31. Schoene, C.; Fierer, J. O.; Bennett, S. P.; Howarth, M. *Angew. Chem. Int. Ed.* **2014**, *53* (24), 6101-6104.
32. Stammaes, J.; Fleckenstein, B.; Sollid, L. M. *Biochim. Biophys. Acta* **2008**, *1784* (11), 1804-1811.
33. Rothlisberger, D.; Khersonsky, O.; Wollacott, A. M.; Jiang, L.; DeChancie, J.; Betker, J.; Gallaher, J. L.; Althoff, E. A.; Zanghellini, A.; Dym, O.; Albeck, S.; Houk, K. N.; Tawfik, D. S.; Baker, D. *Nature* **2008**, *453* (7192), 190-195.
34. Sternberg, S. H.; Redding, S.; Jinek, M.; Greene, E. C.; Doudna, J. A. *Nature* **2014**, *507* (7490), 62-67.
35. Roach, P. *Nature* **2011**, *478* (7370), 463-464.
36. Chen, I.; Dorr, B. M.; Liu, D. R. *Proc. Natl. Acad. Sci. U. S. A.* **2011**, *108* (28), 11399-11404.
37. Parthasarathy, R.; Subramanian, S.; Boder, E. T. *Bioconjug. Chem.* **2007**, *18* (2), 469-476.
38. Nguyen, G. K.; Kam, A.; Loo, S.; Jansson, A. E.; Pan, L. X.; Tam, J. P. *J. Am. Chem. Soc.* **2015**, *137* (49), 15398-15401.
39. Yang, R.; Wong, Y. H.; Nguyen, G. K. T.; Tam, J. P.; Lescar, J.; Wu, B. *J. Am. Chem. Soc.* **2017**, *139* (15), 5351-5358.
40. Zhang, W. B.; Sun, F.; Tirrell, D. A.; Arnold, F. H. *J. Am. Chem. Soc.* **2013**, *135* (37), 13988-13997.
41. Brune, K. D.; Leneghan, D. B.; Brian, I. J.; Ishizuka, A. S.; Bachmann, M. F.; Draper, S. J.; Biswas, S.; Howarth, M. *Sci. Rep.* **2016**, *6*, 19234.
42. Rosen, C. B.; Kwant, R. L.; MacDonald, J. I.; Rao, M.; Francis, M. B. *Angew. Chem. Int. Ed.* **2016**, *55* (30), 8585-8589.
43. Goldenberg, D. P.; Creighton, T. E. *J. Mol. Biol.* **1983**, *165* (2), 407-413.
44. Rebello, S.; Jose, L.; Sindhu, R.; Aneesh, E. M. *Appl. Microbiol. Biotechnol.* **2017**, *101* (7), 2677-2689.

45. Yumura, K.; Akiba, H.; Nagatoishi, S.; Kusano-Arai, O.; Iwanari, H.; Hamakubo, T.; Tsumoto, K. *J. Biochem.* **2017**, *162* (3), 203-210.
46. Sun, F.; Zhang, W. B.; Mahdavi, A.; Arnold, F. H.; Tirrell, D. A. *Proc. Natl. Acad. Sci. U. S. A.* **2014**, *111* (31), 11269-11274.
47. Botyanszki, Z.; Tay, P. K.; Nguyen, P. Q.; Nussbaumer, M. G.; Joshi, N. S. *Biotechnol. Bioeng.* **2015**, *112* (10), 2016-2024.
48. Brune, K. D.; Buldun, C. M.; Li, Y.; Taylor, I. J.; Brod, F.; Biswas, S.; Howarth, M. *Bioconjug. Chem.* **2017**, *28* (5), 1544-1551.
49. Fairhead, M.; Howarth, M. *Methods Mol. Biol.* **2015**, *1266*, 171-184.
50. Keeble, A. H.; Banerjee, A.; Ferla, M. P.; Reddington, S. C.; Anuar, I. N. A. K.; Howarth, M. *Angew. Chem. Intl. Ed.* **2017**, *56* (52), 16521-16525.
51. Shcherbo, D.; Murphy, C. S.; Ermakova, G. V.; Solovieva, E. A.; Chepurnykh, T. V.; Shcheglov, A. S.; Verkhusha, V. V.; Pletnev, V. Z.; Hazelwood, K. L.; Roche, P. M.; Lukyanov, S.; Zarausky, A. G.; Davidson, M. W.; Chudakov, D. M. *Biochem. J.* **2009**, *418* (3), 567-574.
52. Dumon-Seignovert, L.; Cariot, G.; Vuillard, L. *Protein Expr. Purif.* **2004**, *37* (1), 203-206.
53. Assenberg, R.; Delmas, O.; Graham, S. C.; Verma, A.; Berrow, N.; Stuart, D. I.; Owens, R. J.; Bourhy, H.; Grimes, J. M. *Acta Crystallogr. F* **2008**, *64* (Pt 4), 258-262.
54. Davis, I. W.; Leaver-Fay, A.; Chen, V. B.; Block, J. N.; Kapral, G. J.; Wang, X.; Murray, L. W.; Arendall, W. B., 3rd; Snoeyink, J.; Richardson, J. S.; Richardson, D. C. *Nucleic Acids Res.* **2007**, *35* (Web Server issue), W375-383.
55. Altschul, S. F.; Madden, T. L.; Schaffer, A. A.; Zhang, J.; Zhang, Z.; Miller, W.; Lipman, D. J. *Nucleic Acids Res.* **1997**, *25* (17), 3389-3402.
56. Edgar, R. C. *BMC Bioinformatics* **2004**, *5*, 113.
57. Li, W.; Godzik, A. *Bioinformatics* **2006**, *22* (13), 1658-1659.

## Table of Contents graphic

